



*Citation for published version:*

Shaharum, NSN, Shafri, HZM, Ghani, WAWAK, Samsatli, S, Al-Habshi, MMA & Yusuf, B 2020, 'Oil Palm Mapping Over Peninsular Malaysia Using Google Earth Engine and Machine Learning Algorithms', *Remote Sensing Applications: Society and Environment*, vol. 17, 100287. <https://doi.org/10.1016/j.rsase.2020.100287>

*DOI:*

[10.1016/j.rsase.2020.100287](https://doi.org/10.1016/j.rsase.2020.100287)

*Publication date:*

2020

*Document Version*

Peer reviewed version

[Link to publication](#)

*Publisher Rights*

CC BY-NC-ND

**University of Bath**

**Alternative formats**

If you require this document in an alternative format, please contact:  
[openaccess@bath.ac.uk](mailto:openaccess@bath.ac.uk)

**General rights**

Copyright and moral rights for the publications made accessible in the public portal are retained by the authors and/or other copyright owners and it is a condition of accessing publications that users recognise and abide by the legal requirements associated with these rights.

**Take down policy**

If you believe that this document breaches copyright please contact us providing details, and we will remove access to the work immediately and investigate your claim.

## Manuscript Details

<b>Manuscript number</b>	RSASE_2019_318_R1
<b>Title</b>	Oil Palm Mapping Over Peninsular Malaysia Using Google Earth Engine and Machine Learning Algorithms
<b>Article type</b>	Research Paper

### Abstract

Oil palm plays a pivotal role in the ecosystem, environment, economy and without proper monitoring, uncontrolled oil palm activities could contribute to deforestation that can cause high negative impacts on the environment and therefore, proper management and monitoring of the oil palm industry are necessary. Mapping the distribution of oil palm is crucial in order to manage and plan the sustainable operations of oil palm plantations. Remote sensing provides a means to detect and map oil palm from space effectively. Recent advances in cloud computing and big data allow rapid mapping to be performed over large a geographical scale. In this study, 30 m Landsat 8 data were processed using a cloud computing platform of Google Earth Engine (GEE) in order to classify oil palm land cover using non-parametric machine learning algorithms such as Support Vector Machine (SVM), Classification and Regression Tree (CART) and Random Forest (RF) for the first time over Peninsular Malaysia. The hyperparameters were tuned, and the overall accuracy produced by the SVM, CART and RF were 93.16%, 80.08% and 86.50% respectively. Overall, the SVM classified the 7 classes (water, built-up, bare soil, forest, oil palm, other vegetation and paddy) the best. However, RF extracted oil palm information better than the SVM. The algorithms were compared and the McNemar's test showed significant values for comparisons between SVM and CART and RF and CART. On the other hand, the performance of SVM and RF are considered equally effective. Despite the challenges in implementing machine learning optimisation using GEE over a large area, this paper shows the efficiency of GEE as a cloud-based free platform to perform bioresource distributions mapping such as oil palm over a large area in Peninsular Malaysia.

**Keywords** cloud computing; Landsat; oil palm

**Corresponding Author** Helmi Shafri

**Corresponding Author's Institution** Universiti Putra Malaysia (UPM)

**Order of Authors** Nur Shafira Nisa Shaharum, Helmi Shafri, Wan Azlina Wan Ab Karim Ghani, Sheila Samsatli, Mohammed Al-Habshi, Badronnisa Yusuf

1  
2  
3  
4 **Oil Palm Mapping Over Peninsular Malaysia Using Google Earth Engine**  
5 **and Machine Learning Algorithms**  
6  
7

8 Nur Shafira Nisa Shaharum<sup>a</sup>, Helmi Zulhaidi Mohd Shafri<sup>a,b\*</sup>, Wan Azlina Wan  
9 Ab Karim Ghani<sup>c</sup>, Sheila Samsatli<sup>d</sup>, Mohammed Mustafa Abdulrahman Al-  
10 Habshi<sup>a</sup> and Badronnisa Yusuf<sup>a</sup>  
11  
12

13  
14 *<sup>a</sup>Department of Civil Engineering, Faculty of Engineering, Universiti Putra Malaysia, 43400,*  
15 *UPM Serdang, Selangor, Malaysia; <sup>b</sup>Geospatial Information Science Research Centre*  
16 *(GISRC), Faculty of Engineering, Universiti Putra Malaysia (UPM), 43400 Serdang,*  
17 *Selangor, Malaysia; <sup>c</sup>Department of Chemical and Environmental Engineering/Sustainable*  
18 *Process Engineering Research Centre (SPERC), Faculty of Engineering, Universiti Putra*  
19 *Malaysia, 43400, UPM Serdang, Selangor, Malaysia; <sup>d</sup>Department of Chemical Engineering,*  
20 *University of Bath, Claverton Down, BA2 7AY, United Kingdom.*  
21

22 Corresponding author: [helmi@upm.edu.my](mailto:helmi@upm.edu.my)  
23  
24  
25  
26  
27  
28  
29  
30  
31  
32  
33  
34  
35  
36  
37  
38  
39  
40  
41  
42  
43  
44  
45  
46  
47  
48  
49  
50  
51  
52  
53  
54  
55  
56  
57  
58  
59

# Oil Palm Mapping Over Peninsular Malaysia using Google Earth Engine and Machine Learning Algorithms

## Abstract

Oil palm plays a pivotal role in the ecosystem, environment, economy and without proper monitoring, uncontrolled oil palm activities could contribute to deforestation that can cause high negative impacts on the environment and therefore, proper management and monitoring of the oil palm industry are necessary. Mapping the distribution of oil palm is crucial in order to manage and plan the sustainable operations of oil palm plantations. Remote sensing provides a means to detect and map oil palm from space effectively. Recent advances in cloud computing and big data allow rapid mapping to be performed over large a geographical scale. In this study, 30 m Landsat 8 data were processed using a cloud computing platform of Google Earth Engine (GEE) in order to classify oil palm land cover using non-parametric machine learning algorithms such as Support Vector Machine (SVM), Classification and Regression Tree (CART) and Random Forest (RF) for the first time over Peninsular Malaysia. The hyperparameters were tuned, and the overall accuracy produced by the SVM, CART and RF were 93.16%, 80.08% and 86.50% respectively. Overall, the SVM classified the 7 classes (water, built-up, bare soil, forest, oil palm, other vegetation and paddy) the best. However, RF extracted oil palm information better than the SVM. The algorithms were compared and the McNemar's test showed significant values for comparisons between SVM and CART and RF and CART. On the other hand, the performance of SVM and RF are considered equally effective. Despite the challenges in implementing machine learning optimisation using GEE over a large area, this paper shows the efficiency of GEE as a cloud-based free platform to perform bioresource distributions mapping such as oil palm over a large area in Peninsular Malaysia.

Keywords: cloud computing; image classification; Landsat; machine learning; oil palm

## 1. Introduction

Malaysia is a Southeast Asian country sharing borders with Thailand, Indonesia and Brunei. Malaysia is a tropical country with two geographical regions: Peninsular Malaysia and Borneo (Sabah and Sarawak). It experiences a humid, hot and rainy climate throughout the year, experiencing temperature ranging between 23°C – 32°C throughout the country. This

119  
120  
121 allows Malaysia to generate income from agricultural crop activities such as paddy  
122  
123 cultivation, rubber and oil palm planting (Fahmi et al. 2013; Nambiappan et al. 2018). Among  
124  
125 the agricultural crops, oil palm produces the highest amount of biomass, and as one of the  
126  
127 largest palm oil exporters in the world, the total number oil palms planted in Malaysia  
128  
129 reached over 5 million hectares (ha) in 2017 (Ng et al. 2012). Moreover, oil palm was the  
130  
131 main contributor of agricultural crops to the country's GDP in 2017 with a total contribution  
132  
133 of 46.6% (Mahidin 2018). Despite its benefits, oil palm activities contributed to massive  
134  
135 deforestation and caused negative impacts to the environment (Fitzherbert et al. 2008) and  
136  
137 therefore, oil palm activities have been labelled as the main threat to the earth by contributing  
138  
139 to the global warming and climate change (Shuit et al. 2009). Destroying wildlife habitats and  
140  
141 forests for planting oil palm trees have worsened the negative implications. Even though  
142  
143 palm oil can be used as a renewable energy source and help contribute to the 17 Sustainable  
144  
145 Development Goals as presented by the United Nations, it is important to note that the  
146  
147 environment will be in jeopardy without proper management and monitoring on the oil palm  
148  
149 industry, which will in turn affect environmental sustainability. However, managing huge  
150  
151 areas of oil palm plantations will be challenging. Furthermore, implementing ground surveys  
152  
153 or other traditional survey methods will require a tremendous amount of time, effort and high  
154  
155 cost. A number of people are required to execute data collection over a large area and  
156  
157 therefore, high computational power will be essential to process such big data. Hence, the  
158  
159 utilisation of remote sensing is a suitable and a cost-effective method for collecting data  
160  
161 covering a huge area.  
162  
163  
164

165  
166 The use of remote sensing for oil palm applications can be found in many publications  
167  
168 using a variety of sensors, platforms and algorithms. For example, Thenkabail et al. (2004)  
169  
170 used four bands with 4 m of spatial resolution from IKONOS to carry out a study on oil palm  
171  
172 biomass estimations and carbon stock calculations. Before implementing image  
173  
174  
175  
176  
177

178  
179  
180 classification, the band was first masked by extracting the oil palm feature from non-oil

181 palms. Next, Gutiérrez-Vélez and DeFries (2013) utilised MODIS data with 250 m of pixel  
182 size and successfully produced an oil palm map covering an area of 939,204 km<sup>2</sup>. Another  
183 similar study using MODIS data was conducted on a larger study area covering several  
184 regions in Southeast Asia including Peninsular Malaysia, Sumatra, Java, Borneo, Sulawesi  
185 and Mindanao. The study has successfully classified a total of 13 classes together with  
186 mangrove forests, rainforests and large-scale palm plantations (Miettinen et al. 2012). This  
187 indicated that studies using coarse spatial resolution can be implemented in oil palm studies.  
188 On the other hand, using higher spatial resolution data, analysis on oil palm studies can be  
189 improved and more information can be extracted. Jusoff and Pathan (2009) and Shafri and  
190 Hamdan (2009) used hyperspectral sensor to map individual oil palm trees. A more subtle  
191 analysis was conducted by Shafri et al. (2011) via Maximum Likelihood Classifier (MLC)  
192 and successfully detected Ganoderma disease infections in the plantations with an overall  
193 accuracy of 82%. More recently, the high spectral resolution as provided by hyperspectral  
194 data has allowed Camacho et al. (2019) to successfully produce an oil palm map  
195 distinguishing healthy from diseased palm trees.  
196  
197  
198  
199  
200  
201  
202  
203  
204  
205  
206  
207  
208  
209  
210  
211  
212  
213

214 In terms of classification algorithms, Morel et al. (2012) have successfully  
215 distinguished between forest and oil palm areas on Landsat data using k-means and MLC  
216 algorithms. Then, Glinskis and Gutiérrez-Vélez (2019) used MLC algorithm to classify oil  
217 palm and successfully categorised it into 3 stages (infant palm, juvenile palm and adult palm)  
218 via Sentinel 1 and 2 data. Studies using more advanced algorithms or approaches such as  
219 Support Vector Machine (SVM), Random Forest (RF), Deep Learning, Artificial Neural  
220 Network (ANN) and other machine learning algorithms to classify oil palm land cover tend to  
221 produce better results (Nooni et al. 2014; Li et al. 2015; Lee et al. 2016; Noi and Kappas  
222 2018). For example, Cheng et al. (2016) performed land cover classifications on Landsat and  
223  
224  
225  
226  
227  
228  
229  
230  
231  
232  
233  
234  
235  
236

237  
238  
239 ALOS-PALSAR remote sensing data via SVM and Minimum Distance algorithms. The  
240  
241 classifications were applied on two different sites, and the overall accuracies produced by  
242  
243 SVM were higher than Minimum Distance for both Landsat and ALOS-PALSAR data.  
244  
245 Cheng et al. (2018) expanded the oil palm classification on larger areas covering Malaysia,  
246  
247 Indonesia, Thailand, Nigeria and Ghana using ALOS-PALSAR data. The study achieved an  
248  
249 overall accuracy of more than 94% for all the aforementioned countries. **A review of studies**  
250  
251 **on fusion techniques between optical and radar data to map land use was conducted by Joshi**  
252  
253 **et al (2016) and it showed that fusion techniques are efficient for cloud issue. De Alban et al**  
254  
255 **(2018) combined Landsat and L-band Synthetic Aperture Radar (SAR) data to carry out land**  
256  
257 **use land cover change application in tropical landscapes. A machine learning RF algorithm**  
258  
259 **was used to classify the land use and the accuracy obtained was 92.96% to 93.83%. However,**  
260  
261 **fusion technique requires large amount of time and data to produce the cloud-free image.**

262  
263  
264  
265 As shown above, there have been several oil palm studies using various remote  
266  
267 sensing data, however, most of the studies were limited to small areas (Li et al. 2016; Chong  
268  
269 et al. 2017; Charters et al. 2019; Fawcett et al. 2019) and utilised personal computers,  
270  
271 requiring the ability to store data and perform image processing using remote sensing  
272  
273 software that were mostly commercial. Data obtained from the impacts of oil palm activities  
274  
275 that were conducted on small areas are not suitable and insufficient to be used for measuring  
276  
277 the sustainability level for a huge area, especially for the whole country. On the other hand,  
278  
279 the utilisation of very high-resolution images on big areas will be costly in addition to  
280  
281 requiring high computational power which will be essential to process the data. Even so, GEE  
282  
283 cloud computing provides an alternative to process huge amount of geospatial data with zero  
284  
285 cost and without the need to personally store the data on the personal computer. Sidhu et al.  
286  
287 (2018) performed land cover change analysis in Singapore's landmass via GEE and the result  
288  
289 showed that the forest cover was affected by the monsoon cycles. Another study by Oliphant  
290  
291  
292  
293  
294  
295

296  
297  
298 et al. (2019) to map cropland over Southeast and Northeast Asia via Landsat was carried out  
299  
300 using GEE, but no specific crops (e.g. oil palm, paddy and others) are mapped. In Malaysia,  
301  
302 first ever effort to map oil palm over the Peninsular Malaysia using cloud computing platform  
303  
304 was done using the Remote Ecosystem Monitoring Assessment Pipeline (REMAP) tool as  
305  
306 conducted by Shaharum et al. (2019). However, it was limited to only the use of RF  
307  
308 classifier, limiting the investigation of the performance of other machine learning algorithms.  
309  
310 Furthermore, as the toolbox is not programmable, the parameters of the classifier cannot be  
311  
312 optimized or tuned accordingly. In addition, the imagery data used in REMAP was fixed and  
313  
314 cannot be filtered to produce the best cloud-free data. In addition, the GEE algorithms were  
315  
316 run in code editor module, allowing more optimization parameters to be tested for  
317  
318 classification. To the best of our knowledge, there has been no report on the utilisation of  
319  
320 GEE for oil palm mapping over the entire Peninsular Malaysia. Hence, this study was  
321  
322 conducted to test the capability of 30 m Landsat data using the GEE cloud computing  
323  
324 platform and compare machine learning algorithms such as SVM, CART and RF to map oil  
325  
326 palm land cover over Peninsular Malaysia covering an area of 132,265 km<sup>2</sup>. Even though  
327  
328 there are many available remote sensing data and techniques available to classify the oil palm  
329  
330 plantation, selecting the best technique will be vital.  
331  
332  
333

## 334 335 **2. Material and Methods**

### 336 337 **2.1 Study area**

338  
339 Malaysia is located between Thailand, Singapore and Indonesia. It comprises of two regions:  
340  
341 Peninsular Malaysia and Borneo (Sabah and Sarawak). This study covers Peninsular  
342  
343 Malaysia (N 4°00'0.00", E 102°29'59.99"; Fig 1) or West Malaysia with an approximate land  
344  
345 area of 132,265 km<sup>2</sup>. Malaysia is a tropical country experiencing both hot and humid weather  
346  
347  
348  
349  
350  
351  
352  
353  
354



355  
356  
357 throughout the year. The temperature ranges between 23°C – 32°C and during hot weather,  
358  
359 the temperature can exceed over 40°C (Shahar 2016).  
360  
361  
362  
363  
364

365 [Figure 1 near here]  
366  
367  
368

## 369 **2.2 Google Earth Engine**

370  
371  
372 Vast amount of the geospatial remote sensing data provided in the GEE has allowed the  
373  
374 powerful cloud-based platform to be used in various studies involving deforestation, oil palm  
375  
376 plantations, environmental assessment, change detection and urban classifications (Patel et al.  
377  
378 2015; Dong et al. 2016; Goldblatt et al. 2016; Shelestov et al. 2017). GEE can be accessed  
379  
380 either through Application Programming Interface (API) or web-based Interactive  
381  
382 Development Environment (IDE) (Gorelick et al. 2017). The data catalog provided in the  
383  
384 GEE houses a multi-petabyte accessible geospatial dataset that is made up of Earth-observing  
385  
386 remote sensing images, including Landsat, MODIS, Sentinel-1 and Sentinel-2.  
387  
388  
389  
390  
391

392 [Figure 2 near here]  
393  
394  
395

396 Figure 2 shows the GEE platform via Javascript API and it allows the user to control the data  
397  
398 through coding. The user can write the programs using client libraries in Python and  
399  
400 Javascript (programming languages). Furthermore, the client libraries provide objects for  
401  
402 Images, Collections and other data types. In fact, the user can perform various remote sensing  
403  
404 analyses in the GEE API platform such as image classifications, multitemporal urban extents,  
405  
406 post-processing and object detection. Enormous amount of Earth Engine public data catalog  
407  
408 provided in the cloud-based GEE platform helps the user to process very large geospatial  
409  
410  
411  
412  
413

414  
415  
416 datasets without having to suffer the information technology pains including the need of high  
417  
418 computational power resources and huge amount of storage.  
419  
420  
421  
422

### 423 424 **2.3 Data collection and pre-processing**

425  
426  
427 The availability of 30 m Landsat 8 images for the study area were obtained from the United  
428  
429 States Geological Survey through the GEE platform (Roy et al. 2014). The images were  
430  
431 already being pre-processed and corrected at Top-Of-Atmosphere (TOA) reflectance as  
432  
433 explained by Chander et al. (2009) by converting at sensor (spectral radiance) to  
434  
435 exoatmospheric TOA reflectance. The benefits of using images that have been corrected at  
436  
437 TOA reflectance are it compensates for different values of the exoatmospheric solar  
438  
439 irradiance occur from spectral band differences and the TOA reflectance can eliminate the  
440  
441 cosine effect of different solar zenith angles due to the time difference between data  
442  
443 acquisitions. Also, it corrects the dissimilarity in the Earth–Sun distance between different  
444  
445 data acquisition dates.  
446  
447  
448  
449  
450

451 [Table 1 near here]  
452  
453  
454  
455

456 This study utilised only 7 bands of Landsat 8 with 30 m spatial resolution (see Table 1).  
457  
458 Landsat 8 data is obtained via passive remote sensing, and it is sensitive towards clouds.  
459  
460 Several Landsat 8 images taken from year 2016 and 2017 were patched together to attain the  
461  
462 missing information that were blocked by the clouds. The existence of clouds can affect the  
463  
464 quality of the remote sensing data and furthermore, the information beneath the cloud will be  
465  
466 unclassified. The utilisation of commercial remote sensing software to perform image  
467  
468 patching on a huge area consumes significant resources and time (Gambo et al. 2018;  
469  
470  
471  
472

473  
474  
475 Shaharum et al. 2018). However, the GEE platform allows the user to perform data  
476  
477 acquisition and image patching in a few seconds. Furthermore, it allows the user to set the  
478  
479 percentage of the cloud cover and the desired date of the satellite data to be used.  
480  
481

### 482 **3. Methodology**

483  
484  
485 Several geospatial datasets were utilised in this study to produce the oil palm land cover maps  
486  
487 over Peninsular Malaysia: (i) 30 m Landsat 8 data from 2016 to 2017 (7 original bands) (ii)  
488  
489 Shuttle Radar Topographic Mission (SRTM), Digital Elevation Model (DEM), (iii)  
490  
491 Additional data including NDVI, Normalised Difference Water Index (NDWI) and others.  
492  
493  
494 The workflow adapted for this study is shown in Figure 3.  
495

496  
497 [Figure 3 near here]  
498

499  
500 This study compared 3 different machine learning algorithms (SVM, RF and CART), and a  
501  
502 total of 7 classes including oil palm were classified. The importance of oil palm plantation  
503  
504 has been discussed in the introduction and therefore, this study focuses on producing oil palm  
505  
506 land cover map. Moreover, the land cover map produced can later be used in the next study to  
507  
508 assess the impacts of oil palm plantation over Peninsular Malaysia.  
509

#### 510 **3.1 Data used for classification**

511  
512  
513 As illustrated in Table 1, a total of 7 bands obtained from Landsat 8 images were used and  
514  
515 these bands were used to generate additional data (see Table 2). A number of equations were  
516  
517 used to produce additional data that will be included together with the other 7 bands to be  
518  
519 used in the image classification stage.  
520  
521

522  
523 [Table 2 near here]  
524  
525  
526  
527  
528  
529  
530  
531

532  
533  
534 The layers in Table 2 were stacked together with Landsat 8 bands (Table 1) to be used in the  
535 classification process. These additional layers are capable of extracting a certain information  
536 in a more efficient way. For example, NDVI is derived from the ratio between Red and Near-  
537 infrared (NIR) reflectance bands. Furthermore, NDVI is sensitive towards chlorophyll  
538 content and the green leaf density. The presence of chlorophyll in green vegetations absorbs  
539 in the red band. Hence, NDVI is useful to extract information of the green vegetations on the  
540 ground (Bro-Jørgensen et al. 2008).  
541  
542  
543  
544  
545  
546  
547  
548  
549  
550  
551

### 552 **3.2 Sampling**

553  
554 Samples were created in the GEE platform and a total of 7 classes were identified: water,  
555 built-up, bare soil, oil palm, forest, other vegetation and paddy. The samples were created  
556 using the point format for every state in Peninsular Malaysia, covering a total of 11 states via  
557 random sampling. The samples were created with the aid of land cover map provided by the  
558 Department of Agriculture (DOA) and high-resolution Google Earth images as shown in  
559 Figure 4(a). The samples were then divided into two components: training and testing. A total  
560 of 70% from the whole created samples (4307 points) were used to classify the Landsat  
561 images and the remaining 30% of the samples (1846 points) were used to validate and assess  
562 the accuracy of the algorithms used. The classification and validation were done in GEE and  
563 the accuracy assessment was calculated using the common confusion matrix method.  
564  
565  
566  
567  
568  
569  
570  
571  
572  
573  
574  
575  
576  
577  
578

579 [Figure 4 near here]  
580  
581  
582  
583  
584  
585  
586  
587  
588  
589  
590

### 3.3 Supervised machine learning algorithms

#### 3.3.1 Support Vector Machine

Supervised classification can be conducted using machine learning and non-machine learning algorithms. SVM is a type of supervised machine learning algorithm that works well in classification and regression. It uses a hyperplane (see Figure 5) to divide the support vectors to distinctly classify the data points, and there are many possible ways for the hyperplane to separate the support vectors in which, the main objective of SVM is to find the hyperplane that has the maximum margin (separate support vectors of both classes at a maximum distance) (Maxwell et al. 2018).

[Figure 5 near here]

SVM comprises of several hyperparameters: kernel type, gamma and penalty value. These hyperparameters can be tuned and adjusted to improve the performance of SVM in image classification.

#### 3.3.2 Classification and Regression Tree

The CART is similar to DT. CART, which is a type of supervised machine learning algorithm that forms a binary decision tree. It involves the identification and construction of the tree using the training samples for which the correct classification is unknown. The decision tree starts with a root node derived from any variable in the feature space and minimises a measure of the impurity of the two sibling nodes (see Figure 6). Then, the decision tree grows by means of the successive subdivisions until it reaches a stage where

650  
651  
652 there is no significant reduction in the measure of impurity when further division is  
653  
654 implemented (Bittencourt and Clarke 2003; Jiang et al. 2010).  
655  
656  
657  
658  
659

660 [Figure 6 near here]  
661  
662  
663

664 The decision tree is made of multilevel and multi-leaf nodes and the decision tree will  
665  
666 undergo a pruning process once it is constructed. The constructed trees are often over-fit  
667  
668 because an excessive number of nodes and branches are often being created. Therefore, the  
669  
670 tree can be pruned by controlling the parameters or thresholds for the new branches (Calbury  
671  
672 2016).  
673  
674

### 675 676 3.3.3 Random Forest 677

678 RF or Random Decision Forest is a non-parametric machine learning algorithm that can be  
679  
680 used in both classification and regression analysis. It is a type of ensemble learning algorithm  
681  
682 that ensembles a number of decision trees and forms a forest (see Figure 7). This algorithm  
683  
684 combines random features or a combination of features at each node to grow a tree. The  
685  
686 bagging method is used in this algorithm to generate the training samples, and each selected  
687  
688 feature is drawn randomly by the replacement of N (size of original training set) examples.  
689  
690 The examples are classified based on the highest voted class produced from all the trees in  
691  
692 the forest (Pal 2005).  
693  
694  
695  
696  
697  
698

699 [Figure 7 near here]  
700  
701  
702  
703  
704  
705  
706  
707  
708

709  
710  
711 One of the most frequently used attributes in the decision tree induction is the Gini Index. For  
712 a given training set  $T$ , selecting one case (pixel) at random and assuming that it belongs to  
713 some class  $C_i$ , the expression can be written as:  
714  
715  
716

$$\sum_{j \neq i} (f(C_i, T)/|T|)((f(C_j, T)/|T|) \quad (1)$$

717  
718  
719  
720  
721 where  $f(C_i, T)/|T|$  is the probability that the selected case belongs to class  $C_i$ . Gini Index acts  
722 as an attribute selection measure in RF that measures the impurity of an attribute with respect  
723 to the classes. Since RF works by assembling a number of trees, whereby  $N$  is to form a  
724 forest, the value of  $N$  can be defined by the user to get the best output of the classification.  
725  
726 The RF algorithm can use a large number of trees in the ensemble and as a result, it works  
727 well in high dimensional data (Gislason et al. 2006).  
728  
729  
730  
731  
732  
733  
734

#### 735 736 3.3.4 Hyperparameters optimisation 737

738 Every algorithm has its own built-in hyperparameters/parameters that can be adjusted and  
739 further tuned to improve its performance. A hyperparameter is a parameter which contains a  
740 value that is set or defined before performing any learning process, and different model  
741 training algorithms consist of different hyperparameters. In this study, the hyperparameters in  
742 SVM, CART and RF algorithms were optimised in GEE, and the involved hyperparameters  
743 were tabulated in Table 3.  
744  
745  
746  
747  
748  
749  
750  
751

752 [Table 3 near here]  
753  
754  
755  
756

757 These hyperparameters are tuneable and can directly affect the robustness of the learning  
758 models, thus optimisation of the hyperparameters is required to achieve the best performance  
759 level of the algorithms. The identification of the hyperplane in SVM can be due to the type of  
760 kernel,  $k$ : Linear, Radial basis function, Polynomial and Sigmoid. Kernels are used to solve a  
761  
762  
763  
764  
765  
766  
767

768  
769  
770 non-linear problem in a higher dimension and is usually referred to as kernel trick (Afonja  
771 2017). Gamma,  $g$  is the hyperparameter in SVM that defines how far the influence of a  
772 single training example reaches. A high value of gamma considers only nearby points (near  
773 identified hyperplane) in the calculation. Conversely, low gamma considers far away points  
774 to be included in the calculation for the separation of the hyperplane (Patel 2017). As for the  
775 penalty or regularisation hyperparameter,  $C$  in SVM is to avoid misclassification in the  
776 learning model. A larger value of  $C$  tells SVM to produce a smaller-margin hyperplane and  
777 on the contrary, a small value of  $C$  enlarges the margin of the hyperplane.  
778  
779  
780  
781  
782  
783  
784  
785  
786  
787  
788  
789  
790

791 [Figure 8 near here]

792  
793 In this study, a total of four hyperparameters were fine-tuned in CART. Firstly, the cross-  
794 validation factor,  $cv$  in CART partitions of the training samples were tuned into  $K$  (number of  
795 folds) equally sized subsamples. Assuming that the training samples were divided into 10  
796 folds of subsamples, 9 of the subsamples are used as training data and the other 1 subsample  
797 as validation as shown in Figure 8 (Ivanovic 2016). Then, max depth,  $d$  is used to determine  
798 the maximum of the tree depth in the model. The number of terminal nodes increases  
799 proportionally to the depth of the tree. For  $d$  equals to 1 will have 2 terminal nodes, and  $d$   
800 equals to 2 will have a maximum of 4 nodes. The maximum of the nodes in a tree depends on  
801 the depth of the tree by implementing the rule of 2 to the power of  $d$  (Molnar 2016).  
802  
803  
804  
805  
806  
807  
808  
809  
810  
811  
812  
813  
814  
815  
816  
817  
818  
819  
820  
821  
822  
823  
824  
825  
826



### 3.4 McNemar's test

McNemar's test is a statistical test that applies to 2 x 2 contingency table. Sometimes, it is known as McNemar's Chi-Square test because it has a chi-square distribution. McNemar's test is conducted to determine whether if there are differences on a dichotomous dependent variable between two related classifiers or groups (Pal et al. 2013). The McNemar's test has been used by Yu et al. (2017) to determine the difference between classifications based on other pairs of features. Duro et al. (2012) performed McNemar's test to compare the classification results between DT, RF and SVM via object-based and pixel-based techniques. The result showed that the p-value via object-based was statistically significant ( $p < 0.05$ ) when comparing DT with either RF or SVM. On the other hand, no statistically significant difference ( $p > 0.05$ ) was produced when comparing the results obtained from different algorithms via pixel-based technique.

## 4. Results and Discussion

### 4.1 Land cover classifications

This study was aimed to produce an oil palm land cover map over Peninsular Malaysia by comparing SVM, CART and RF machine learning algorithms in the GEE platform. A total of 7 classes (water, built-up, bare soil, forest, oil palm, other vegetation and paddy) were classified. However, the classification output analysis emphasized only on oil palm because the produced oil palm map will later be used to evaluate the spatial distribution of oil palm in Peninsular Malaysia and will be included into a Geographic Information System (GIS) database for further analysis. The hyperparameters were optimised and classified maps produced by the algorithms are shown in Figure 9.

886  
887  
888 [Figure 9 near here]  
889  
890  
891  
892

893 The hyperparameters optimisation was carried out in the GEE. A grid search method was  
894 implemented for each algorithm to find the best hyperparameters to be used for the  
895 classification (Gupta et al. 2018). Generally, the hyperparameters used to produce the outputs  
896 for each algorithm are as shown in Table 3.  
897  
898  
899  
900

901  
902 In this study, 7 classes were identified in which, water classified features with water elements  
903 such as lakes, sea, rivers and ponds. Built-up classified buildings, metals, concretes and  
904 roads. Then, bare soil classified features that are bare land, open areas and places full of sand  
905 or soil (such as construction site). Oil palm classified oil palm trees while other vegetation  
906 classified features other than oil palm and forests such as shrubs, other crops and plantations.  
907 Since the aim of this study was to test the performance of machine learning algorithms to  
908 extract oil palm plantation from 30 m Landsat 8 images in the cloud-based, GEE platform,  
909 additional information such as NDVI, NDWI and slope were included to enhance the  
910 classification, especially in distinguishing one class from another. The produced oil palm map  
911 provides the information on the oil palm distribution for 2017 and furthermore, the map can  
912 later be used in the future studies such as to evaluate the impact of oil palm land cover in  
913 detailed.  
914  
915  
916  
917  
918  
919  
920  
921  
922  
923  
924  
925  
926  
927  
928  
929  
930

#### 931 **4.2 Overall accuracies and land cover maps comparison**

932

933 A total of 30% of testing samples (water: 213, built-up: 311, bare soil: 126, forest: 470, oil  
934 palm: 331, other vegetation: 276 and paddy: 119) were used to validate the classified land  
935 cover maps, and the overall accuracies obtained for each state were calculated (see Table 4).  
936  
937  
938  
939

940 The total area of oil palm in Peninsular Malaysia produced by CART, RF and SVM were  
941  
942  
943  
944

945  
946  
947 3005758 ha, 2795287 ha and 2924434 ha respectively. Table 4 indicates that SVM produced  
948  
949 the highest overall accuracy with an average of 93.16%. That is followed by the overall  
950  
951 accuracies produced by RF and CART with an average of 86.50% and 80.08% respectively.  
952  
953  
954 The overall accuracies produced were calculated via confusion matrix based on the  
955  
956 accuracies of the 7 classified classes.  
957  
958  
959  
960  
961  
962  
963  
964  
965  
966  
967  
968  
969  
970  
971  
972  
973  
974  
975  
976  
977  
978  
979  
980  
981  
982  
983  
984  
985  
986  
987  
988  
989  
990  
991  
992  
993  
994  
995  
996  
997  
998  
999  
1000  
1001  
1002  
1003

1004  
1005  
1006  
1007  
1008  
1009  
1010  
1011  
1012  
1013  
1014  
1015  
1016  
1017  
1018  
1019  
1020  
1021  
1022  
1023  
1024  
1025  
1026  
1027  
1028  
1029  
1030  
1031  
1032  
1033  
1034  
1035  
1036  
1037  
1038  
1039  
1040  
1041  
1042  
1043  
1044

[Table 4 near here]

1045  
1046  
1047  
1048  
1049  
1050  
1051  
1052  
1053  
1054  
1055  
1056  
1057  
1058  
1059  
1060  
1061  
1062  
1063  
1064  
1065  
1066  
1067  
1068  
1069  
1070  
1071  
1072  
1073  
1074  
1075  
1076  
1077  
1078  
1079  
1080  
1081  
1082  
1083  
1084  
1085

[Table 5 near here]

1086  
1087  
1088  
1089 By referring to the inventory provided by the Malaysia Palm Oil Board (MPOB), the area of  
1090  
1091 oil palm plantations produced by SVM, CART and RF were compared for each state in  
1092  
1093 Peninsular Malaysia. Table 5 shows the difference of oil palm area produced by SVM, CART  
1094  
1095 and RF by comparing the generated results with the MPOB inventory. However, the  
1096  
1097 limitation of 30 m coarse resolution data, RF, CART and SVM have overestimated the oil  
1098  
1099 palm area and misclassified other classes as oil palm land cover. Based on the classified oil  
1100  
1101 palm areas tabulated in Table 5, most of the states overestimated the oil palm areas. Kedah  
1102  
1103 overestimated more than 60000 ha and followed by Selangor with an overestimation of more  
1104  
1105 than 56000 ha of oil palm area. Then, the result showed that at least 1000 ha of land area was  
1106  
1107 misclassified as oil palm in Perlis. This is because the misclassified pixels were due to the  
1108  
1109 similarity of the reflectance value of the pixels. Therefore, the pixels that were misclassified  
1110  
1111 as oil palms have contributed to the overestimation of the oil palm area for the  
1112  
1113 aforementioned states. Conversely, all three algorithms underestimated the oil palm area for  
1114  
1115 Melaka. Overall, all the machine learning algorithms, SVM, RF and CART overestimated the  
1116  
1117 oil palm area for Peninsular Malaysia. Although SVM produced the highest overall accuracy,  
1118  
1119 RF produced the least errors in comparison with the MPOB inventory in oil palm  
1120  
1121 classification by producing an overall error of 0.03%, followed by SVM and CART with  
1122  
1123 0.08% and 0.11% for the whole oil palm area of Peninsular Malaysia respectively.  
1124  
1125 Furthermore, RF classified oil palm land cover and produced the nearest result (oil palm area)  
1126  
1127 to the MPOB inventory for most of the states: Negeri Sembilan, Pulau Pinang, Kedah,  
1128  
1129 Pahang, Perak, Perlis and Terengganu. Then, CART extracted the most accurate oil palm  
1130  
1131 areas for Johor and Kelantan, and SVM extracted the best for Melaka.  
1132  
1133  
1134  
1135  
1136  
1137

1138 This study had tested the performance of three algorithms (CART, RF and SVM) with  
1139  
1140 fine-tuned hyperparameters on 30 m Landsat data, and managed to produce oil palm land  
1141  
1142  
1143  
1144

1145  
1146  
1147 cover maps over Peninsular Malaysia using a cloud-based platform, GEE. The powerful  
1148  
1149 cloud computing platform, GEE has made mapping oil palm land cover over Peninsular  
1150  
1151 Malaysia using Landsat data possible. However, this study has confronted a few setbacks.  
1152  
1153 Firstly, the utilisation of 30 m spatial resolution data might produce errors due to mixed  
1154  
1155 pixels and furthermore, there might be more than one class in a single pixel. Then, the  
1156  
1157 similarity of the reflectance between other vegetation and oil palm as well as between bare  
1158  
1159 soil and built-up had caused confusion in the classification. Furthermore, the images used  
1160  
1161 were the result from image patching, in which the product might contain errors in the pixels,  
1162  
1163 hence reducing the quality of the image. Peninsular Malaysia is a huge area, and to obtain a  
1164  
1165 single cloud-free image for a tropical region covering such huge area is merely impossible.  
1166  
1167 Thus, image patching is one of the alternatives to obtain an almost cloud-free data. Therefore,  
1168  
1169 it is challenging to ensure the quality of optical data, especially when it involves huge tropical  
1170  
1171 area.  
1172  
1173  
1174  
1175  
1176  
1177  
1178  
1179  
1180  
1181  
1182  
1183  
1184  
1185  
1186  
1187  
1188  
1189  
1190  
1191  
1192  
1193  
1194  
1195  
1196  
1197  
1198  
1199  
1200  
1201  
1202  
1203

[Figure 10 near here]

1204  
1205  
1206  
1207  
1208  
1209  
1210  
1211  
1212  
1213  
1214  
1215  
1216  
1217  
1218  
1219  
1220  
1221  
1222  
1223  
1224  
1225  
1226  
1227  
1228  
1229  
1230  
1231  
1232  
1233  
1234  
1235  
1236  
1237  
1238  
1239  
1240  
1241  
1242  
1243  
1244

[Figure 11 near here]



1245  
1246  
1247  
1248  
1249  
1250  
1251  
1252  
1253  
1254  
1255  
1256  
1257  
1258  
1259  
1260  
1261  
1262  
1263  
1264  
1265  
1266  
1267  
1268  
1269  
1270  
1271  
1272  
1273  
1274  
1275  
1276  
1277  
1278  
1279  
1280  
1281  
1282  
1283  
1284  
1285  
1286  
1287  
1288  
1289  
1290  
1291  
1292  
1293  
1294  
1295  
1296  
1297  
1298  
1299  
1300  
1301  
1302  
1303

Figures 10 and 11 are the selected focused regions in Pulau Pinang and Selangor respectively that were classified by CART, RF and SVM. The feature (in the red box) showed in Figure 10(a) is oil palm trees. Based on the classified images (Figures 10(b), 10(c) and 10(d)), the result showed that SVM misclassified most of the oil palm pixels as other vegetation. Furthermore, SVM misinterpreted the bare soil pixels with built-up in Selangor as shown in Figure 11(d). On the other hand, the oil palm and bare soil pixels for both areas (Selangor and Pulau Pinang) were found to be well classified by CART and RF. These findings showed that the utilisation of additional layers (NDVI, NDWI and others) in the tree methods implemented in RF and CART is more efficient. In addition, both tree-based algorithms (RF and CART) can classify the pixels better than the SVM that works via maximizing the hyperplane. Moreover, the failure of SVM algorithm in separating the support vectors had led to classification errors. As for RF and CART, the RF algorithm has improved the classification as the trees in the RF were ensembled into a forest, and finally the classes were defined based on the majority vote. Although Figures 10 and 11 showed that SVM misclassified oil palm and bare soil pixels, the best algorithm to classify all the 7 classes for the whole Peninsular Malaysia is SVM. However, by comparing all three machine learning algorithms, this study agreed that RF extracted oil palm class the best for the whole Peninsular Malaysia.

### 4.3 McNemar's test

McNemar's test has been carried out in this study to measure the significance between the classification of SVM and CART, SVM and RF and CART and RF. The 2 x 2 contingency table as tabulated in Table 6 was used to calculate the p-values.

[Table 6 near here]

The null hypothesis of this test states that the probability of Test 1 being correctly classified is equal to the probability of Test 2 being correctly classified. Also, the probability of Test 1 being incorrectly classified is equal to the probability of Test 2 being incorrectly classified. In other words,  $P_a + P_b = P_a + P_c$  or  $P_b + P_d = P_c + P_d$ , which leads to  $P_b = P_c$ .

$P_a$  = Probability of Test 1 being positive and Test 2 being positive  
 $P_b$  = Probability of Test 1 being positive and Test 2 being negative  
 $P_c$  = Probability of Test 1 being negative and Test 2 being positive  
 $P_d$  = Probability of Test 1 being negative and Test 2 being negative

The p-value will be calculated and the value of  $p < 0.05$  is considered as a significant result, thus rejecting the null hypothesis. In this study, calculations of the p-value using the formula demonstrated by Foody (2004) were conducted for all the algorithms and the results are tabulated in Table 8.

[Table 7 near here]

The p-value obtained when comparing between SVM and RF is 0.28 ( $p > 0.05$ ), while the other two comparisons obtained values of  $p < 0.05$ . Due to the robustness and powerful machine learning algorithms, SVM and RF algorithms can classify the pixels well. Hence, the comparison between SVM and RF gave a non-significant p-value  $> 0.05$  and thus, accepted the null hypothesis.

## 5. Conclusion

In this study, we utilised 30 m Landsat data in the GEE platform to produce oil palm land cover maps over Peninsular Malaysia. The GEE platform is controllable and it provides

1363  
1364  
1365 options especially in selecting the processing methods, algorithms and data input.  
1366  
1367 Furthermore, it allows users to design the workflow based on their needs. In this study, three  
1368 machine learning algorithms were used and the hyperparameters were tuned. Accuracy  
1369 assessments for the classified maps were conducted using high-resolution Google Earth  
1370 images and the map provided by the DOA. The comparison of the classified oil palm areas  
1371 with the inventory provided by MPOB has shown that there is a large uncertainty of oil palm  
1372 land cover in Perlis, Kedah and Selangor. Overall, CART, SVM and RF were able to classify  
1373 the land cover maps and produced acceptable results by producing an overall accuracy of  
1374 80.08%, 93.16% and 86.50% respectively. Then, McNemar's test was conducted and it  
1375 showed that significant p-values were obtained when comparing CART to both SVM and RF.  
1376 However, the test showed a non-significant value when comparing between RF and SVM.  
1377 This shows that both methods can reliably be used to produce high accuracy maps in GEE  
1378 and later be used to classify other crops. Moving on, such timely and high accuracy estimates  
1379 of oil palm areas could be embedded with other ancillary GIS data for a variety of monitoring  
1380 and decision-making applications, including yield prediction, supply-chain logistics,  
1381 commodity markets, bioenergy estimation and more.

1382  
1383  
1384  
1385  
1386  
1387  
1388  
1389  
1390  
1391  
1392  
1393  
1394  
1395  
1396  
1397  
1398  
1399  
1400  
1401  
1402 GEE provides various geospatial data including Sentinel 2, Sentinel 1 and MODIS.  
1403  
1404 The utilisation of higher spatial resolution data such as Sentinel 2 with 20 m to 10 m of pixel  
1405 size can be tested to improve the classification. Moreover, Sentinel 1 works with active  
1406 sensors, and it is suitable to be used on tropical regions. The integration of Sentinel 1 data in  
1407 the GEE platform can reduce the time needed to process huge amounts of radar data. On top  
1408 of that, there are many more methods available in GEE to pre-process remote sensing data, in  
1409 which some methods might produce good results and able to improve the accuracy of the  
1410  
1411  
1412  
1413  
1414  
1415  
1416  
1417  
1418  
1419  
1420  
1421

1422  
1423  
1424 data. In addition, the programmable platform produces the possibilities for the cloud  
1425  
1426 computing GEE to be integrated with the powerful deep learning methods.  
1427  
1428  
1429  
1430

## 1431 **Acknowledgements**

1432  
1433 We would like to thank Universiti Putra Malaysia for their facilities and support for this research.  
1434 Sponsorship from the Engineering and Physical Sciences Research Council UK (EPSRC/RCUK)  
1435 (Grant Number: EP/P018165/1- Newton Fund) is gratefully acknowledged. The comments from the  
1436 anonymous reviewers in improving this article are highly appreciated.  
1437  
1438  
1439  
1440  
1441

## 1442 **References**

- 1443  
1444  
1445 Afonja T. 2017. Kernel functions. [accessed 2019 March 12].  
1446 <https://towardsdatascience.com/kernel-function-6f1d2be6091>.  
1447  
1448  
1449  
1450 Belgiu M, Drăguț L. 2016. Random forest in remote sensing: A review of applications and  
1451 future directions. ISPRS J Photogramm Remote Sens. 114:24-31.  
1452 doi:10.1016/j.isprsjprs.2016.01.011.  
1453  
1454  
1455  
1456  
1457 Bittencourt H, Clarke RT. 2003. Use of classification and regression trees (CART) to classify  
1458 remotely-sensed digital images. In: IGARSS 2003. Proceedings of the IEEE Trans  
1459 Geosci Remote Sens Symposium 2003. Toulouse, France, July 21–25: IEEE IGARSS.  
1460 p. 3751–3753.  
1461  
1462  
1463  
1464  
1465  
1466 Brid RS. 2018. Decision trees. Medium; [accessed 2019 January 20].  
1467 [https://medium.com/greyatom/decision-trees-a-simple-way-to-visualize-a-decision-](https://medium.com/greyatom/decision-trees-a-simple-way-to-visualize-a-decision-dc506a403aeb)  
1468 [dc506a403aeb](https://medium.com/greyatom/decision-trees-a-simple-way-to-visualize-a-decision-dc506a403aeb).  
1469  
1470  
1471  
1472  
1473 Bro-Jørgensen J, Brown ME, Pettorelli N. 2008. Using the satellite-derived normalized  
1474 difference vegetation index (NDVI) to explain ranging patterns in a lek-breeding  
1475  
1476  
1477  
1478  
1479  
1480

1481  
1482  
1483 antelope: the importance of scale. *Oecologia*. 158(1):177-182. doi:10.1007/s00442-008-  
1484 1121-z  
1485  
1486  
1487

1488 Calbury. 2016. Object-based Classification: Classification and Regression Tree (CART).  
1489 [Accessed 2019 March 3]. [wiki.landscapetoolbox.org/doku.php/remote\\_sensing\\_](http://wiki.landscapetoolbox.org/doku.php/remote_sensing_methods:classification_and_regression_tree_cart)  
1490 [methods:classification\\_and\\_regression\\_tree\\_cart](http://wiki.landscapetoolbox.org/doku.php/remote_sensing_methods:classification_and_regression_tree_cart).  
1491  
1492  
1493  
1494

1495 Camacho A, Correa CV, Arguello H. 2019. An analysis of spectral variability in hyperspectral  
1496 imagery: a case study of stressed oil palm detection in Colombia. *Int J Remote Sens*.  
1497 40(19):7603-7623. doi:10.1080/01431161.2019.1595210.  
1498  
1499  
1500  
1501

1502 Chander G, Markham BL, Helder DL. 2009. Summary of current radiometric calibration  
1503 coefficients for Landsat MSS, TM, ETM+, and EO-1 ALI sensors. *Remote Sens*  
1504 *Environ*. 113(5):893-903. doi:10.1016/j.rse.2009.01.007.  
1505  
1506  
1507  
1508

1509 Charters LJ, Aplin P, Marston CG, Padfield R, Rengasamy N, Bin Dahalan MP, Evers S. 2019.  
1510 Peat swamp forest conservation withstands pervasive land conversion to oil palm  
1511 plantation in North Selangor, Malaysia. *Int J Remote Sens*.40(19):1-30.  
1512 doi:10.1080/01431161.2019.1574996.  
1513  
1514  
1515  
1516  
1517

1518 Cheng Y, Yu L, Cracknell AP, Gong P. 2016. Oil palm mapping using Landsat and PALSAR:  
1519 A case study in Malaysia. *Int J Remote Sens*. 37(22):5431-5442.  
1520 doi:10.1080/01431161.2016.1241448.  
1521  
1522  
1523  
1524

1525 Cheng Y, Yu L, Xu Y, Lu H, Cracknell AP, Kanniah K, Gong P. 2018. Mapping oil palm  
1526 extent in Malaysia using ALOS-2 PALSAR-2 data. *Int J Remote Sens*. 39(2):432-452.  
1527 doi:10.1080/01431161.2017.1387309.  
1528  
1529  
1530  
1531  
1532  
1533  
1534  
1535  
1536  
1537  
1538  
1539

1540  
1541  
1542 Chong KL, Kanniah KD, Pohl C, Tan KP. 2017. A review of remote sensing applications for  
1543  
1544 oil palm studies. *Geo-spatial Information Science*. 20(2):184-200.  
1545  
1546 doi:10.1080/10095020.2017.1337317.  
1547  
1548

1549 **De Alban, J, Connette G, Oswald P, Webb E. (2018). Combined Landsat and L-band SAR data**  
1550 **improves land cover classification and change detection in dynamic tropical**  
1551 **landscapes. *Remote Sensing*. 10(2):306. doi:10.3390/rs10020306.**  
1552  
1553  
1554  
1555

1556 Dong J, Xiao X, Menarguez MA, Zhang G, Qin Y, Thau D, Biradar C, Moore B. 2016.  
1557  
1558 Mapping paddy rice planting area in northeastern Asia with Landsat 8 images,  
1559  
1560 phenology-based algorithm and Google Earth Engine. *Remote Sens Environ*. 185:142-  
1561  
1562 154. doi:10.1016/j.rse.2016.02.016.  
1563  
1564

1565 Duro DC, Franklin SE, Dubé, MG. 2012. A comparison of pixel-based and object-based image  
1566  
1567 analysis with selected machine learning algorithms for the classification of agricultural  
1568  
1569 landscapes using SPOT-5 HRG imagery. *Remote Sens Environ*. 118:259-272.  
1570  
1571 doi:10.1016/j.rse.2011.11.020.  
1572  
1573

1574 Fahmi Z, Samah BA, Abdullah H. 2013. Paddy industry and paddy farmers well-being: a  
1575  
1576 success recipe for agriculture industry in Malaysia. *Asian Soc Sci*. 9(3):177-181.  
1577  
1578 doi:10.5539/ass.v9n3p177.  
1579  
1580

1581 Fawcett D, Azlan B, Hill TC, Kho LK, Bennie J, Anderson K. 2019. Unmanned aerial vehicle  
1582  
1583 (UAV) derived structure-from-motion photogrammetry point clouds for oil palm (*Elaeis*  
1584  
1585 *guineensis*) canopy segmentation and height estimation. *Int J Remote Sens*. 40(19):1-23.  
1586  
1587 doi:10.1080/01431161.2019.1591651.  
1588  
1589

1590 Fitzherbert EB, Struebig MJ, Morel A, Danielsen F, Brühl CA, Donald PF, Phalan B. 2008.  
1591  
1592 How will oil palm expansion affect biodiversity?. *Trends Ecol Evol*. 23(10):538-545.  
1593  
1594 doi:10.1016/j.tree.2008.06.012.  
1595  
1596  
1597  
1598

- 1599  
1600  
1601 Gambo J, Shafri HZM, Shaharum NSN, Abidin FAZ, Rahman MTA. 2018. Monitoring and  
1602  
1603 Predicting Land Use-Land Cover (LULC) Changes Within and Around Krau Wildlife  
1604 Reserve (KWR) Protected Area in Malaysia Using Multi-Temporal Landsat Data.  
1605  
1606 Geoplanning: journal of geomatics and planning. 5(1):23-44.  
1607  
1608 doi:10.14710/geoplanning.5.1.17-34.  
1609  
1610  
1611  
1612 Gislason PO, Benediktsson JA, Sveinsson JR. 2006. Random forests for land cover  
1613 classification. Pattern Recognit Lett. 27(4):294-300. doi:10.1016/j.patrec.2005.08.011.  
1614  
1615  
1616  
1617 Glinskis EA, Gutiérrez-Vélez VH. 2019. Quantifying and understanding land cover changes  
1618 by large and small oil palm expansion regimes in the Peruvian Amazon. Land Use  
1619 Policy. 80:95-106. doi:10.1016/j.landusepol.2018.09.032.  
1620  
1621  
1622  
1623  
1624 Goldblatt R, You W, Hanson G, Khandelwal A. 2016. Detecting the boundaries of urban areas  
1625 in india: A dataset for pixel-based image classification in google earth engine. Remote  
1626 sensing. 8(8):634. doi:10.3390/rs8080634.  
1627  
1628  
1629  
1630  
1631 Gorelick N, Hancher M, Dixon M, Ilyushchenko S, Thau D, Moore R. 2017. Google Earth  
1632 Engine: Planetary-scale geospatial analysis for everyone. Remote Sens Environ. 202:18-  
1633 27. doi:/10.1016/j.rse.2017.06.031.  
1634  
1635  
1636  
1637  
1638 Gutiérrez-Vélez VH, DeFries R. 2013. Annual multi-resolution detection of land cover  
1639 conversion to oil palm in the Peruvian Amazon. Remote Sens Environ. 129:154-167.  
1640  
1641 doi:10.1016/j.rse.2012.10.033.  
1642  
1643  
1644  
1645 Gupta O, Das AJ, Hellerstein J, Raskar R. 2018. Machine learning approaches for large scale  
1646 classification of produce. Sci Rep. 8(1):5226-5233.  
1647  
1648  
1649  
1650  
1651  
1652  
1653  
1654  
1655  
1656  
1657

1658  
1659  
1660 Ivanovic B. 2016. Cross-validation and decision trees. [accessed 2019 January 15].  
1661  
1662 [https://www.cs.utoronto.ca/~fidler/teaching/2015/slides/CSC411/tutorial3\\_CrossVal-](https://www.cs.utoronto.ca/~fidler/teaching/2015/slides/CSC411/tutorial3_CrossVal-)  
1663 [DTs.pdf](https://www.cs.utoronto.ca/~fidler/teaching/2015/slides/CSC411/tutorial3_CrossVal-DTs.pdf).  
1664  
1665  
1666

1667 Jiang L, Wang W, Yang X, Xie N, Cheng Y. 2010. Classification methods of remote sensing  
1668 image based on decision tree technologies. Paper presented at CCTA 2010. International  
1669 Conference on Computer and Computing Technologies in Agriculture; Oct 20–25;  
1670 Nanchang, China.  
1671  
1672  
1673  
1674  
1675

1676 Joshi N, Baumann M, Ehammer A, Fensholt R, Grogan K, Hostert P, Jepsen MR, Kuemmerie  
1677 T, Meyfroidt P, Mitchard ETA, Reiche J, Ryan CM, Waske B. (2016). A review of the  
1678 application of optical and radar remote sensing data fusion to land use mapping and  
1679 monitoring. *Remote Sensing*. 8(1):70. doi:10.3390/rs8010070.  
1680  
1681  
1682  
1683  
1684

1685 Jusoff K, Pathan M. 2009. Mapping of individual oil palm trees using airborne hyperspectral  
1686 sensing: an overview. *Applied physics research*. 1(1):15-30.  
1687  
1688

1689 Lee JSH, Wich S, Widayati A, Koh LP. 2016. Detecting industrial oil palm plantations on  
1690 Landsat images with Google Earth Engine. *Remote sensing applications: society and*  
1691 *environment*. 4:219-224. doi:10.1016/j.rsase.2016.11.003.  
1692  
1693  
1694  
1695  
1696

1697 Li L, Dong J, Tengku SN, Xiao X. 2015. Mapping oil palm plantations in Cameroon using  
1698 PALSAR 50-m orthorectified mosaic images. *Remote sensing*. 7(2):1206-1224.  
1699 doi:10.3390/rs70201206.  
1700  
1701  
1702  
1703

1704 Li W, Fu H, Yu L, Cracknell A. (2016). Deep learning based oil palm tree detection and  
1705 counting for high-resolution remote sensing images. *Remote Sensing*. 9(1):22.  
1706 doi:https://doi.org/10.3390/rs9010022.  
1707  
1708  
1709  
1710  
1711  
1712  
1713  
1714  
1715  
1716



- 1717  
1718  
1719 Mahidin MU. 2018. Selected Agricultural Indicators Malaysia. Malaysia: Department  
1720 of Statistics Malaysia; [accessed 2019 March 15].  
1721  
1722 [https://www.dosm.gov.my/v1/index.php?r=column/cthemByCat&cat=72&bul\\_id=Uj](https://www.dosm.gov.my/v1/index.php?r=column/cthemByCat&cat=72&bul_id=UjYxeDNkZ0xOUjhFeHpna20wUUJOUT09&menu_id=Z0VTZGU1UHBUT1VJMF1paXRRR0xpdz09)  
1723 [YxeDNkZ0xOUjhFeHpna20wUUJOUT09&menu\\_id=Z0VTZGU1UHBUT1VJMF1pa](https://www.dosm.gov.my/v1/index.php?r=column/cthemByCat&cat=72&bul_id=UjYxeDNkZ0xOUjhFeHpna20wUUJOUT09&menu_id=Z0VTZGU1UHBUT1VJMF1paXRRR0xpdz09)  
1724 [XRRR0xpdz09](https://www.dosm.gov.my/v1/index.php?r=column/cthemByCat&cat=72&bul_id=UjYxeDNkZ0xOUjhFeHpna20wUUJOUT09&menu_id=Z0VTZGU1UHBUT1VJMF1paXRRR0xpdz09).  
1725  
1726  
1727  
1728  
1729  
1730  
1731 Maxwell AE, Warner TA, Fang F. 2018. Implementation of machine-learning classification in  
1732 remote sensing: An applied review. *Int J Remote Sens.* 39(9):2784-2817.  
1733 doi:10.1080/01431161.2018.1433343.  
1734  
1735  
1736  
1737  
1738 Miettinen J, Shi C, Tan WJ, Liew SC. 2012. 2010 land cover map of insular Southeast Asia in  
1739 250-m spatial resolution. *Pattern Recognit Lett.* 3(1):11-20.  
1740 doi:10.1080/01431161.2010.526971.  
1741  
1742  
1743  
1744  
1745 Molnar C. 2016. Interpretable Machine Learning: A Guide for Making Black Box Models  
1746 Explainable. 1<sup>st</sup> ed. Christoph Molnar. [accessed 2019 January 20].  
1747 <https://christophm.github.io/interpretable-ml-book/tree.html>.  
1748  
1749  
1750  
1751  
1752 Morel AC, Fisher JB, Malhi Y. 2012. Evaluating the potential to monitor aboveground biomass  
1753 in forest and oil palm in Sabah, Malaysia, for 2000–2008 with Landsat ETM+ and ALOS-  
1754 PALSAR. *Int J Remote Sens.* 33(11):3614-3639. doi:10.1080/01431161.2011.631949.  
1755  
1756  
1757  
1758  
1759 Nambiappan B, Ismail A, Hashim N, Ismail N, Shahari DN, Idris NAN, Omar N, Salleh KM,  
1760 Hassan NAM, Din AK. 2018. Malaysia: 100 years of resilient palm oil economic  
1761 performance. *J. Oil Palm Res.* 30(1):13-25. doi:10.21894/jopr.2018.0014.  
1762  
1763  
1764  
1765  
1766 Ng WPQ, Lam HL, Ng FY, Kamal M, Lim JHE. 2012. Waste-to-wealth: green potential from  
1767 palm biomass in Malaysia. *J Clean Prod.* 34:57-65. doi:10.1016/j.jclepro.2012.04.004.  
1768  
1769  
1770  
1771  
1772  
1773  
1774  
1775

- 1776  
1777  
1778  
1779  
1780  
1781  
1782  
1783  
1784  
1785  
1786  
1787  
1788  
1789  
1790  
1791  
1792  
1793  
1794  
1795  
1796  
1797  
1798  
1799  
1800  
1801  
1802  
1803  
1804  
1805  
1806  
1807  
1808  
1809  
1810  
1811  
1812  
1813  
1814  
1815  
1816  
1817  
1818  
1819  
1820  
1821  
1822  
1823  
1824  
1825  
1826  
1827  
1828  
1829  
1830  
1831  
1832  
1833  
1834
- Noi PT, Kappas M. 2018. Comparison of random forest, k-nearest neighbor, and support vector machine classifiers for land cover classification using Sentinel-2 imagery. *Sensors*. 18(1):1-20. doi:10.3390/s18010018.
- Nooni IK, Duker AA, Van Duren I, Addae-Wireko L, Osei Jnr EM. 2014. Support vector machine to map oil palm in a heterogeneous environment. *Int J Remote Sens*. 35(13):4778-4794. doi:10.1080/01431161.2014.930201.
- Oliphant AJ, Thenkabail PS, Teluguntla P, Xiong J, Gumma MK, Congalton RG, Yadav K. 2019. Mapping cropland extent of Southeast and Northeast Asia using multi-year time-series Landsat 30-m data using a random forest classifier on the Google Earth Engine Cloud. *Int J Appl Earth Obs Geoinf*. 81:110-124. doi:10.1016/j.jag.2018.11.014.
- Pal M. 2005. Random forest classifier for remote sensing classification. *Int J Remote Sens*. 26(1):217-222. doi:10.1080/01431160412331269698.
- Pal M, Maxwell AE, Warner TA. 2013. Kernel-based extreme learning machine for remote-sensing image classification. *Pattern Recognit Lett*. 4(9):853-862. doi:10.1080/2150704X.2013.805279.
- Patel NN, Angiuli E, Gamba P, Gaughan A, Lisini G, Stevens FR, Tatem AJ, Trianni G. 2015. Multitemporal settlement and population mapping from Landsat using Google Earth Engine. *Int J Appl Earth Obs Geoinf*. 35:199-208. doi:10.1016/j.jag.2014.09.005.
- Patel S. 2017. Chapter 2: SVM (Support Vector Machine) — Theory. [accessed 2019 March 10]. <https://medium.com/machine-learning-101/chapter-2-svm-support-vector-machine-theory-f0812effc72>.
- Roy DP, Wulder MA, Loveland TR, Woodcock CE, Allen RG, Anderson MC, Helder D, Irons JR, Johnson DM, Kennedy R, et al. 2014. Landsat-8: Science and product vision for

1835  
1836  
1837 terrestrial global change research. *Remote Sens Environ.* 145:154-172.  
1838  
1839 doi:10.1016/j.rse.2014.02.001.  
1840  
1841

1842 Shafri HZM, Hamdan N. 2009. Hyperspectral imagery for mapping disease infection in oil  
1843 palm plantation using vegetation indices and red edge techniques. *Am J Appl Sci.*  
1844  
1845 6(6):1031-1035.  
1846  
1847

1848  
1849 Shafri HZM, Anuar MI, Seman IA, Noor NM. 2011. Spectral discrimination of healthy and  
1850  
1851 Ganoderma-infected oil palms from hyperspectral data. *Int J Remote Sens.* 32(22):7111-  
1852  
1853 7129. doi:10.1080/01431161.2010.519003.  
1854  
1855

1856 Shahar FM. 2016 March 18. Heat wave emergency if temperature exceeds 40 degrees Celsius  
1857  
1858 for more than 7 days. *New Straits Times.* [accessed 2019 January 20].  
1859  
1860 [https://www.nst.com.my/news/2016/03/133534/heat-wave-emergency-if-temperature-](https://www.nst.com.my/news/2016/03/133534/heat-wave-emergency-if-temperature-exceeds-40-degrees-celcius-more-7-days)  
1861  
1862 [exceeds-40-degrees-celcius-more-7-days.](https://www.nst.com.my/news/2016/03/133534/heat-wave-emergency-if-temperature-exceeds-40-degrees-celcius-more-7-days)  
1863  
1864

1865 Shaharum NSN, Shafri HZM, Gambo J, Abidin FAZ. 2018. Mapping of Krau Wildlife Reserve  
1866  
1867 (KWR) protected area using Landsat 8 and supervised classification  
1868  
1869 algorithms. *Remote Sensing Applications: Society and Environment.* 10:24-35.  
1870  
1871 doi:10.1016/j.rsase.2018.01.002.  
1872  
1873

1874 Shaharum NSN, Shafri HZM, Ghani WAWAK, Samsatli S, Prince HM, Yusuf B, Hamud AM.  
1875  
1876 2019. Mapping the spatial distribution and changes of oil palm land cover using an open  
1877  
1878 source cloud-based mapping platform. *Int J Remote Sens.* 40(19):1-18.  
1879  
1880 doi:10.1080/01431161.2019.1597311.  
1881  
1882

1883 Shelestov A, Lavreniuk M, Kussul N, Novikov A, Skakun S. 2017. Exploring Google earth  
1884  
1885 engine platform for Big Data Processing: Classification of multi-temporal satellite  
1886  
1887 imagery for crop mapping. *Front Earth Sci.* 5(17):1-10. doi:10.3389/feart.2017.00017.  
1888  
1889  
1890  
1891  
1892  
1893

- 1894  
1895  
1896 Shuit SH, Tan KT, Lee KT, Kamaruddin AH. 2009. Oil palm biomass as a  
1897 sustainable energy source: A Malaysian case study. *Energy*. 34(9):1225-1235.  
1898 doi:10.1016/j.energy.2009.05.008.  
1899  
1900  
1901  
1902  
1903 Sidhu N, Pebesma E, Câmara G. 2018. Using Google Earth Engine to detect land  
1904 cover change: Singapore as a use case. *Eur J Remote Sens*. 51(1):486-500.  
1905 doi:10.1080/22797254.2018.1451782.  
1906  
1907  
1908  
1909  
1910 Thenkabail PS, Stucky N, Griscom BW, Ashton MS, Diels J, Van Der Meer B, Enclona E.  
1911 2004. Biomass estimations and carbon stock calculations in the oil palm plantations of  
1912 African derived savannas using IKONOS data. *Int J Remote Sens*. 25(23):5447-5472.  
1913 doi:10.1080/01431160412331291279.  
1914  
1915  
1916  
1917  
1918  
1919 Yu X, Hyypä J, Litkey P, Kaartinen H, Vastaranta M, Holopainen M. 2017. Single-sensor  
1920 solution to tree species classification using multispectral airborne laser scanning. *Remote*  
1921 *Sensing*. 9(2):108-123. doi:10.3390/rs9020108.  
1922  
1923  
1924  
1925  
1926  
1927  
1928  
1929  
1930  
1931  
1932  
1933  
1934  
1935  
1936  
1937  
1938  
1939  
1940  
1941  
1942  
1943  
1944  
1945  
1946  
1947  
1948  
1949  
1950  
1951  
1952

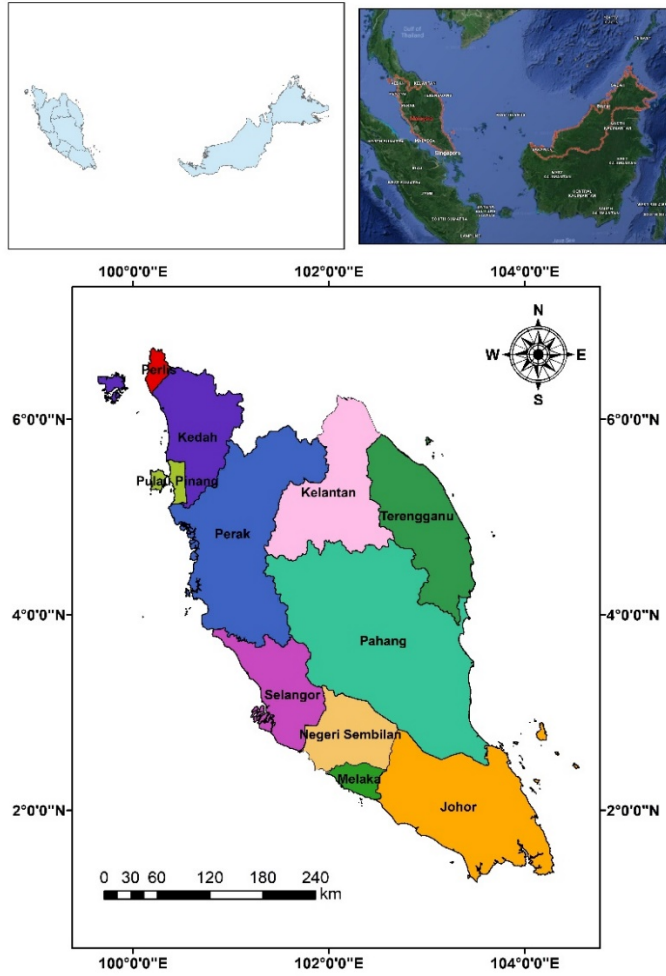


Figure 1. Location of the study area: Peninsular Malaysia.

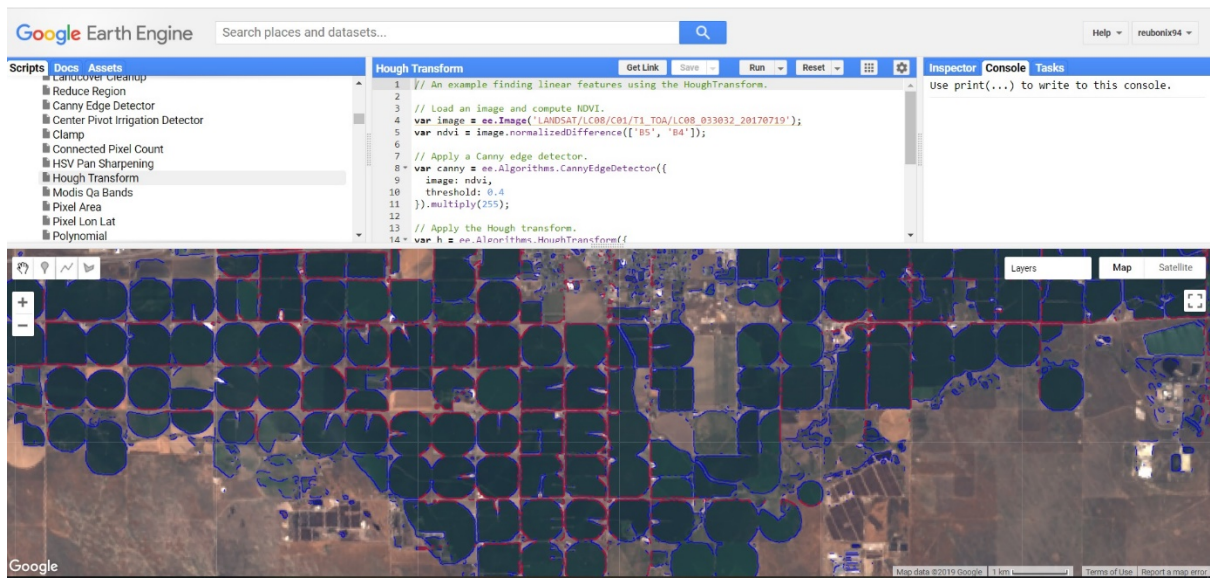


Figure 2. The Earth Engine Javascript API.

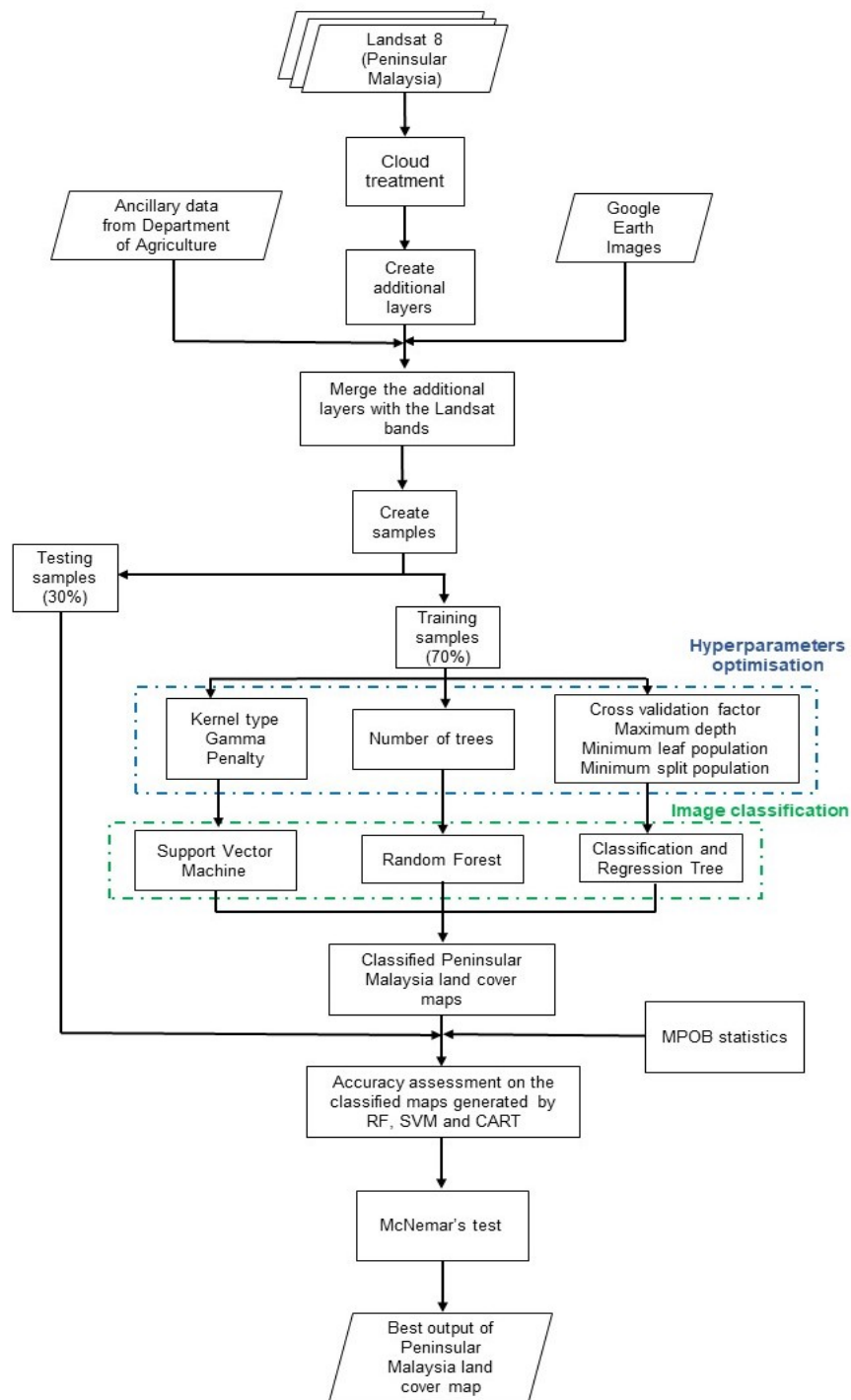


Figure 3. Methodological steps conducted for this study.

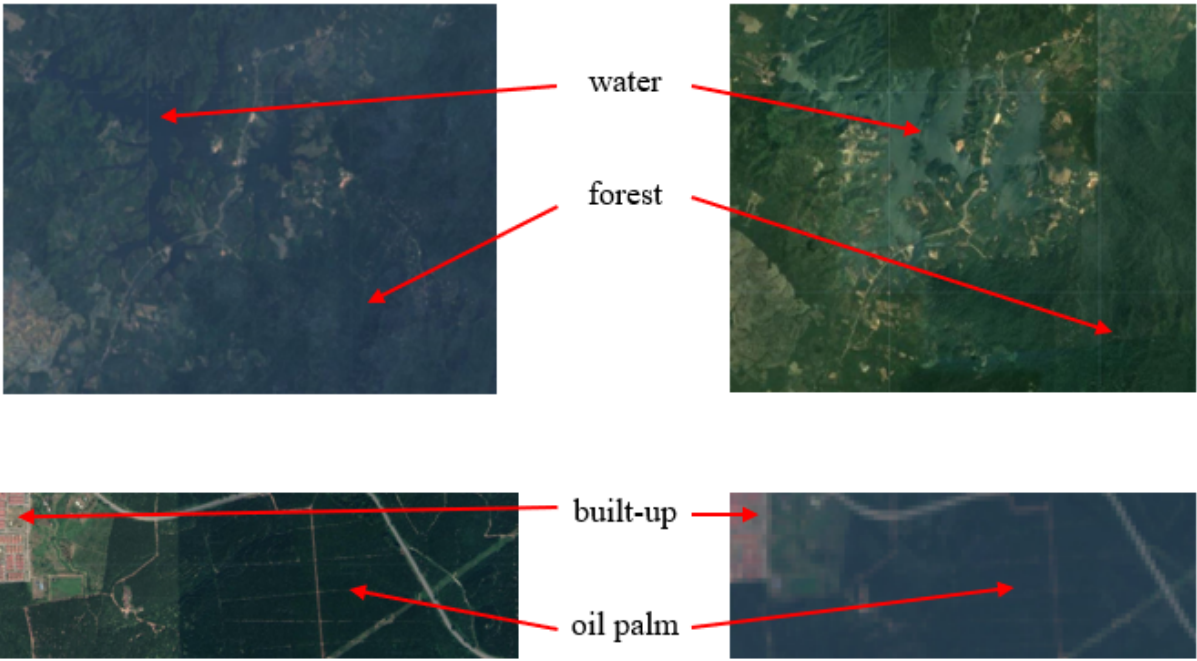


Figure 4. (a) High-resolution Google Earth image, (b) Landsat 8 image.



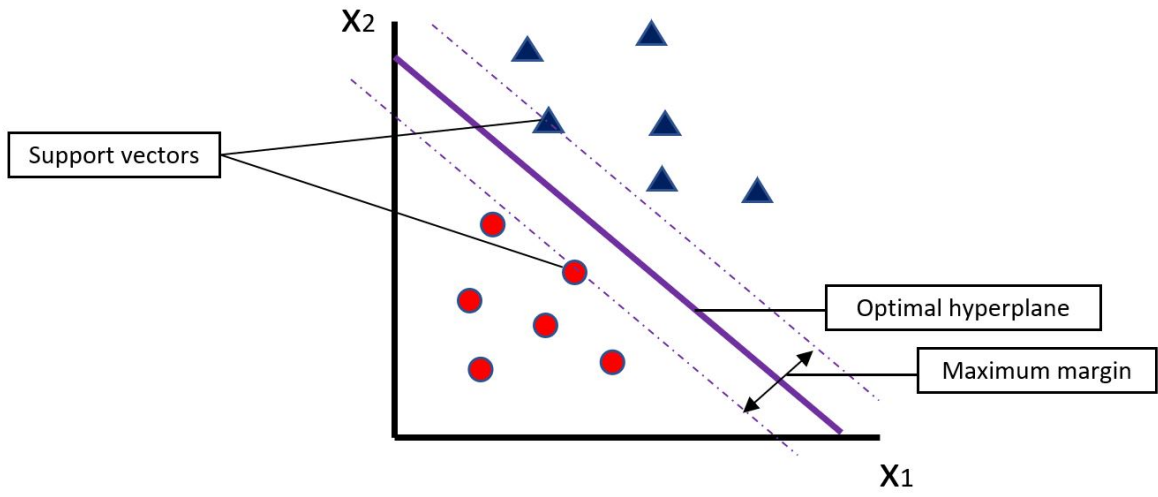


Figure 5. Optimal hyperplane identification in SVM.

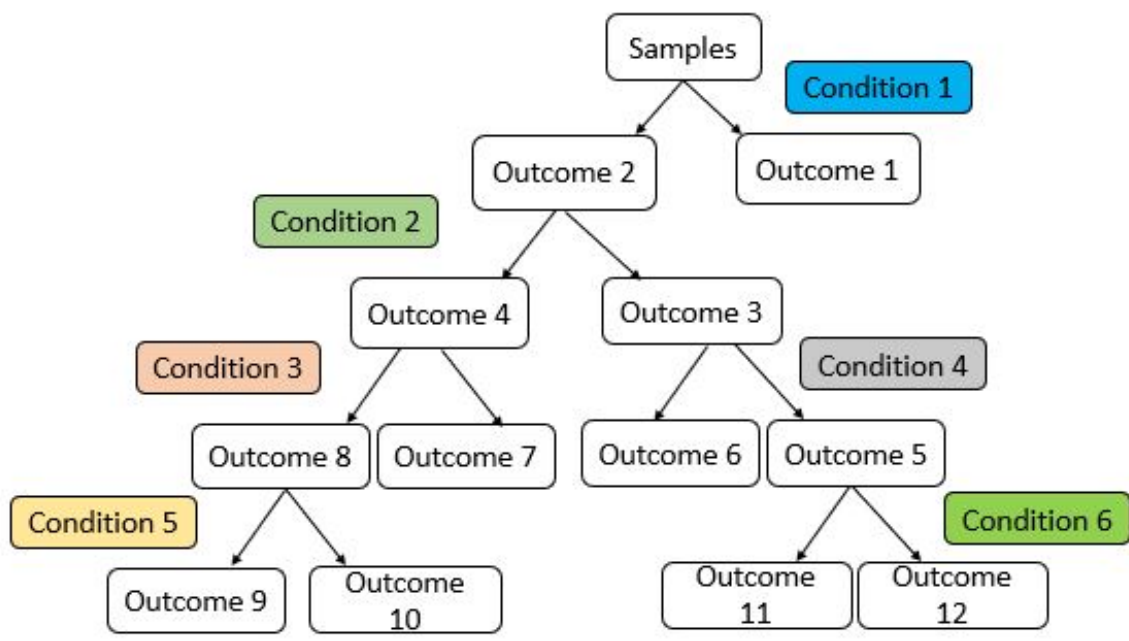


Figure 6. The division of the tree in CART.

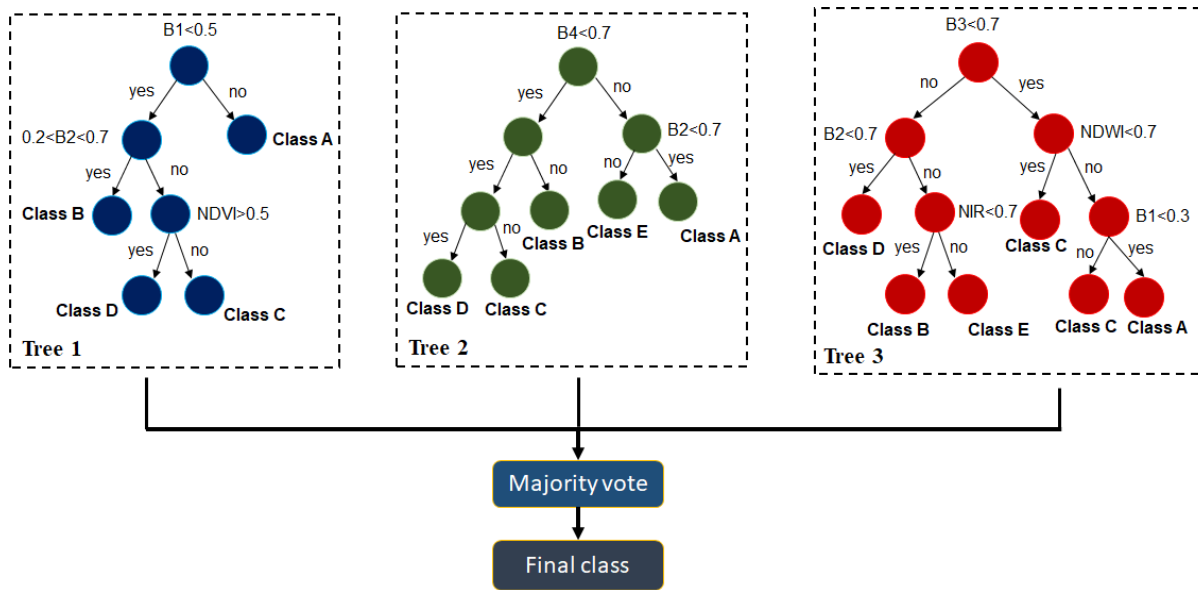


Figure 7. Example of trees ensemble in the RF structure.

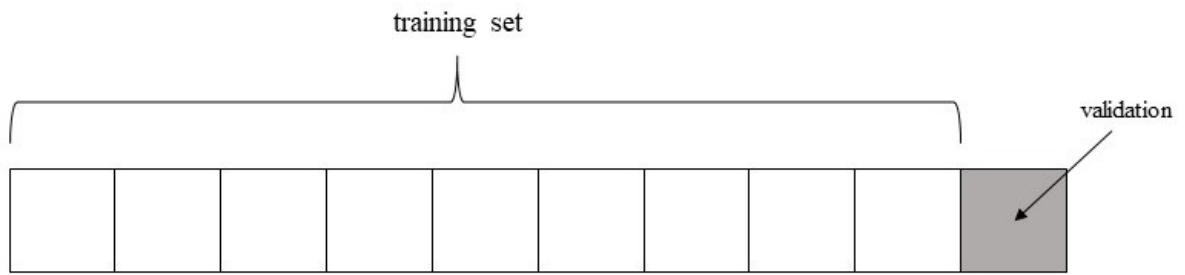


Figure 8. Subsamples in cross validation.

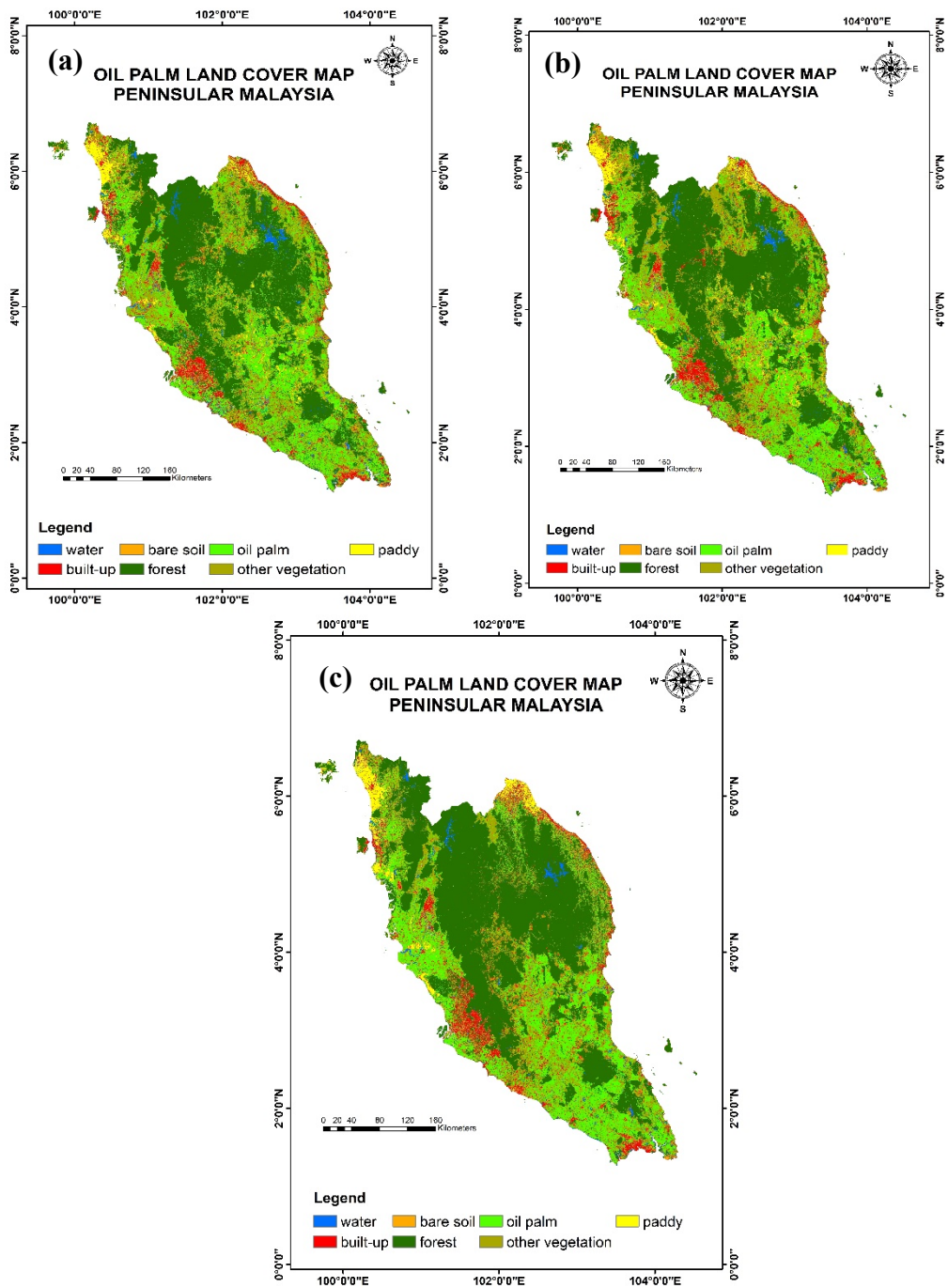


Figure 9. Classified oil palm land cover maps of Peninsular Malaysia, (a) CART, (b) RF and (c) SVM.

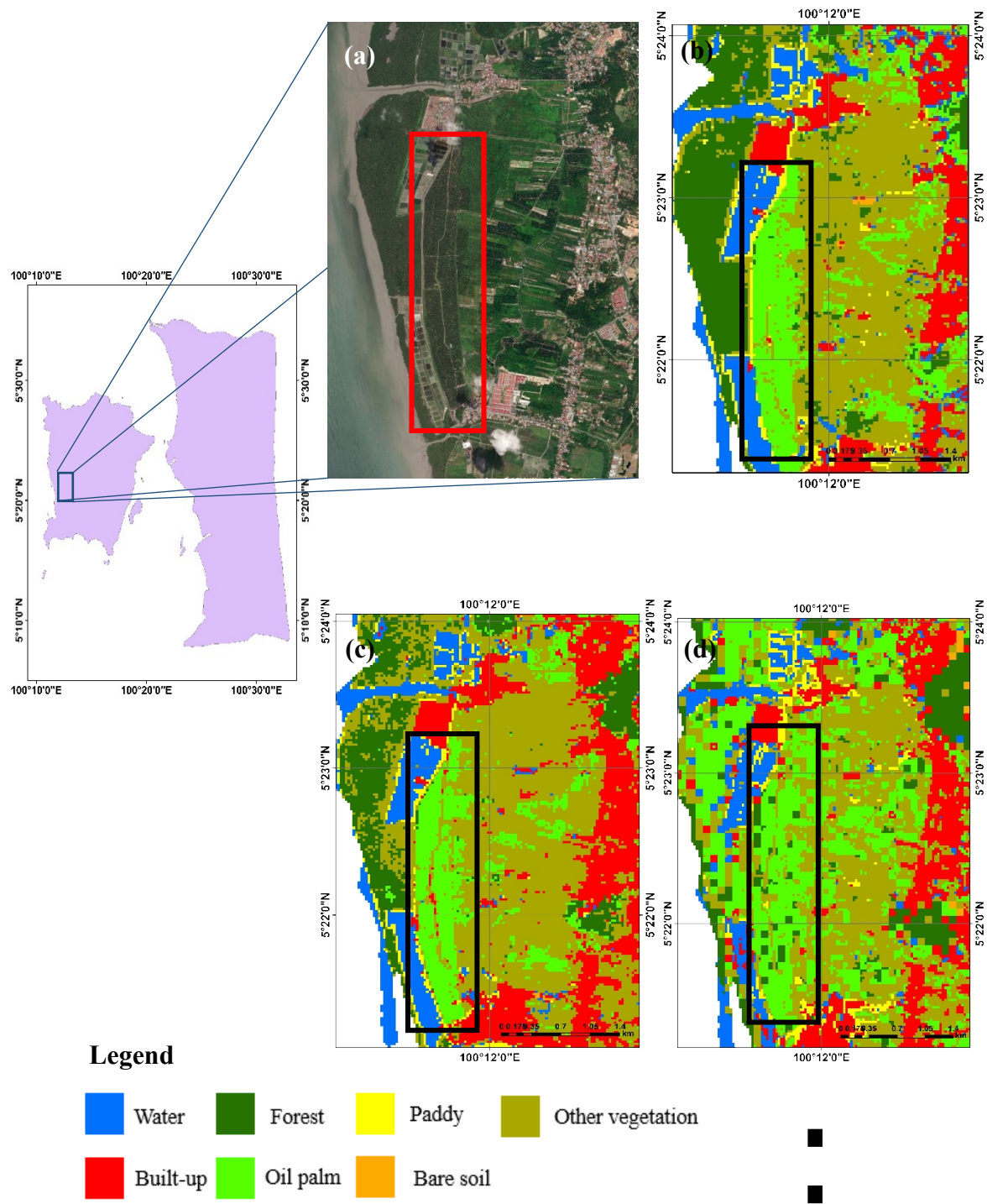


Figure 10. (a) High-resolution Google Earth image, (b) CART, (c) RF and (d) SVM.



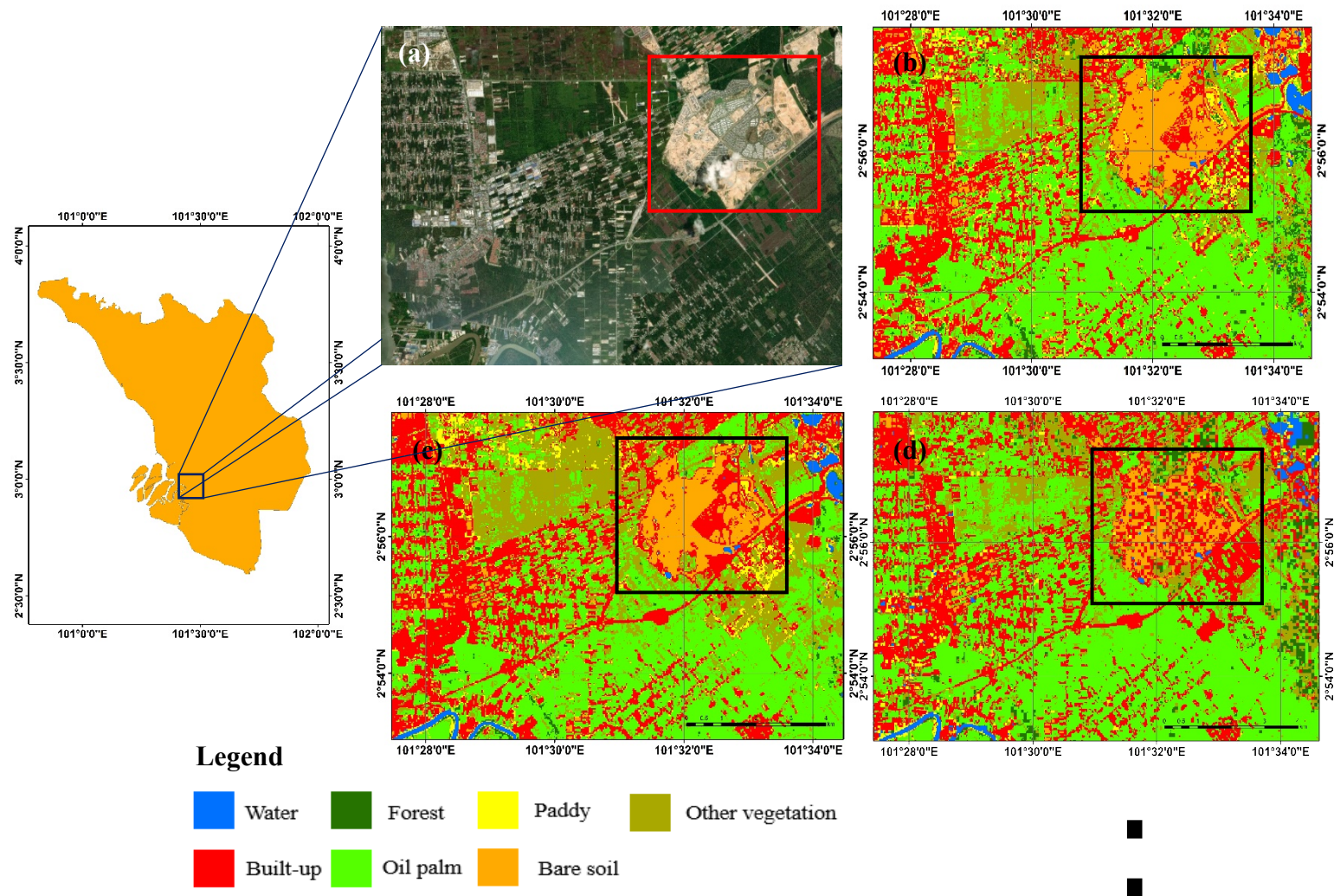


Figure 11. (a) High-resolution Google Earth image, (b) CART, (c) RF and (d) SVM.



Table 1. Information of the Landsat 8 bands.

<b>Name</b>	<b>Description</b>	<b>Pixel size (m)</b>	<b>Wavelength (<math>\mu\text{m}</math>)</b>
Band 1	Coastal aerosol	30	0.435 - 0.451
Band 2	Blue	30	0.452 - 0.512
Band 3	Green	30	0.533 - 0.590
Band 4	Red	30	0.636 - 0.673
Band 5	Near Infrared	30	0.851 - 0.879
Band 6	Short-wave Infrared 1	30	1.566 - 1.651
Band 7	Short-wave Infrared 2	30	2.107 - 2.294

Table 2. Additional layer to be included for classification.

<b>Name</b>	<b>Formula</b>	<b>Reference/Source</b>
NDVI	$\frac{NIR - Red}{NIR + Red}$	(Bannari et al., 1995; Maselli, 2004)
NDWI	$\frac{Green - NIR}{Green + NIR}$	(Xu et al., 2010)
Blue Red	$Blue - Red$	(Murray et al., 2018)
Blue Green	$Blue - Green$	

Table 3. Hyperparameters involved.

<b>Algorithm</b>	<b>Hyperparameter</b>
SVM	Kernel type = Radial Basis Function Gamma = 0.7 Penalty value = 10
CART	Cross validation factor = 5 Max depth = 10 Minimum leaf population = 5 Minimum split population = 10
RF	Number of trees = 30

Table 4. Overall, producer's and user's accuracies for oil palm class of each state and Peninsular Malaysia.

State		Johor	Kedah	Kelantan	Melaka	Negeri Sembilan	Pahang	Pulau Pinang	Perak	Perlis	Selangor	Terengganu	Peninsular Malaysia
RF	OA (%)	89.23	87.85	86.06	85.16	77.57	80.84	89.74	91.30	86.75	89.88	87.10	86.50
	PA (%)	84.62	100.00	89.66	92.00	68.75	80.49	93.10	81.82	85.71	92.45	87.50	86.92
	UA (%)	89.19	84.44	86.67	74.19	75.86	70.21	96.43	90.00	75.00	87.50	80.77	82.75
CART	OA (%)	82.74	86.74	73.94	87.50	78.04	76.64	80.13	82.61	69.88	78.75	83.87	80.08
	PA (%)	84.62	92.11	75.86	96.00	71.88	85.37	65.52	81.82	85.71	73.58	91.67	82.19
	UA (%)	76.74	85.37	73.33	80.00	58.97	70.00	65.52	81.82	50.00	88.64	59.46	71.82
SVM	OA (%)	89.38	97.35	98.18	88.28	88.32	81.28	96.15	97.10	97.59	97.62	93.55	93.16
	PA (%)	89.74	97.22	100.00	92.00	87.50	89.19	96.55	90.91	100.00	98.11	87.50	93.52
	UA (%)	85.37	97.22	93.55	82.14	80.00	76.74	96.55	90.91	100.00	96.30	91.30	90.01

**Note:** OA: Overall accuracy (7 classes); PA: Producer's accuracy (oil palm); UA: User's accuracy (oil palm)

Table 5. Oil palm area produced by RF, CART and SVM in comparison with MPOB.

State	Oil palm area (ha)						
	MPOB	RF		CART		SVM	
		Classified	Difference	Classified	Difference	Classified	Difference
Johor	748860	799142	50282	752133	3273	782282	33422
Kedah	87538	147744	60206	157801	70263	170060	82522
Kelantan	158310	126177	-32133	183388	25078	106969	-51341
Melaka	57372	45768	-11604	42186	-15186	46021	-11351
Negeri Sembilan	184815	184325	-490	195733	10918	194311	9496
Pahang	741495	720745	-20750	802325	60830	717739	-23756
Pulau Pinang	13563	13146	-417	16039	2476	16572	3009
Perak	406469	392518	-13951	445041	38572	528448	121979
Perlis	660	1779	1119	3760	3100	4789	4129
Selangor	137783	196807	59024	195375	57592	194506	56723
Terengganu	171548	167136	-4412	211977	40429	162737	-8811

Table 6. Contingency table.

	<b>Test 2 (positive)</b>	<b>Test 2 (negative)</b>	<b>Row total</b>
<b>Test 1 (positive)</b>	a	b	a + b
<b>Test 1 (negative)</b>	c	d	c + d
<b>Column total</b>	a + c	b + d	n

Table 7. McNemar's test result.

<b>Algorithm 1</b>	<b>Algorithm 2</b>	<b>p-value</b>
SVM	RF	0.28
SVM	CART	0.00
RF	CART	0.00

## Conflict of Interest and Authorship Conformation Form

Please check the following as appropriate:

- All authors have participated in (a) conception and design, or analysis and interpretation of the data; (b) drafting the article or revising it critically for important intellectual content; and (c) approval of the final version.
- This manuscript has not been submitted to, nor is under review at, another journal or other publishing venue.
- The authors have no affiliation with any organization with a direct or indirect financial interest in the subject matter discussed in the manuscript
- The following authors have affiliations with organizations with direct or indirect financial interest in the subject matter discussed in the manuscript:

<b>Author's name</b>	<b>Affiliation</b>
Nur Shafira Nisa Shaharum	Department of Civil Engineering, Faculty of Engineering, Universiti Putra Malaysia, 43400, UPM Serdang, Selangor, Malaysia.
Helmi Zulhaidi Mohd Shafri	Department of Civil Engineering, Faculty of Engineering, Universiti Putra Malaysia, 43400, UPM Serdang, Selangor, Malaysia.  Geospatial Information Science Research Centre (GISRC), Faculty of Engineering, Universiti Putra Malaysia (UPM), 43400 Serdang, Selangor, Malaysia.
Wan Azlina Wan Ab Karim Ghani	Department of Chemical and Environmental Engineering/Sustainable Process Engineering Research Centre (SPERC), Faculty of Engineering, Universiti Putra Malaysia, 43400, UPM Serdang, Selangor, Malaysia.
Sheila Samsatli	Department of Chemical Engineering, University of Bath, Claverton Down, BA2 7AY, United Kingdom.
Mohammed Mustafa Abdulrahman Al-Habshi	Department of Civil Engineering, Faculty of Engineering, Universiti Putra Malaysia, 43400, UPM Serdang, Selangor, Malaysia.
Badronnisa Yusuf	Department of Civil Engineering, Faculty of Engineering, Universiti Putra Malaysia, 43400, UPM Serdang, Selangor, Malaysia.



## **Ethical Statement for Remote Sensing Applications: Society and Environment**

I testify on behalf of all co-authors that our article submitted to Solid State Ionics – Diffusion and Reactions:

**Title:** Oil Palm Mapping Over Peninsular Malaysia Using Google Earth Engine and Machine Learning Algorithms

### **All authors:**

Nur Shafira Nisa Shaharum, Helmi Zulhaidi Mohd Shafri, Wan Azlina Wan Ab Karim Ghani, Sheila Samsatli, Mohammed Mustafa Abdulrahman Al-Habshi and Badronnisa Yusuf.

- 1) this material has not been published in whole or in part elsewhere;
- 2) the manuscript is not currently being considered for publication in another journal;
- 3) all authors have been personally and actively involved in substantive work leading to the manuscript, and will hold themselves jointly and individually responsible for its content.

Date: 3rd Oct 2019

Corresponding author's signature:



6 January 2020

Editor  
Remote Sensing Applications: Society and Environment

Dear Sir,

**SUBMISSION OF AN UPDATED MANUSCRIPT FOR CONSIDERATION OF PUBLICATION IN THE REMOTE SENSING APPLICATIONS: SOCIETY AND ENVIRONMENT JOURNAL**

With reference to the matter as stated above, I would like to submit a manuscript entitled **“Oil Palm Mapping Over Peninsular Malaysia Using Google Earth Engine and Machine Learning Algorithms”** for consideration of publication in the Remote Sensing Applications: Society and Environment Journal. This paper requires improvements after being revised with the decision of minor correction.

We thank the editors and reviewers for the comments to help improve the quality of the manuscript. We have highlighted (using yellow highlighting with red font color) the changes made in our manuscript based on the comments.

The details on the response to the reviewers are given in the correction table for your reference and I hope it will receive a proper evaluation from the Journal reviewers and editors.

Best regards,



Helmi Zulhaidi Mohd Shafri  
Dept. of Civil Engineering  
UPM